Soft Matter

Accepted Manuscript

ROYAL SOCIETY OF CHEMISTRY

www.rsc.org/softmatter

Lysozyme Adsorption in pH-responsive Hydrogel Thin-Films: The non-trivial Role of Acid-Base Equilibrium

Claudio F. Narambuena,[1,3,⊥] Gabriel S. Longo,[2,⊥] Igal Szleifer[1,3,4,*]

[1]Department of Biomedical Engineering, Northwestern University, Evanston, IL, USA; [2]Instituto de Investigaciones Fisicoquímicas Teóricas y Aplicadas (INIFTA), CONICET, La Plata, Argentina; [3]Chemistry of Life Processes Institute, Northwestern University, Evanston, IL, USA; [4]Department of Chemistry, Northwestern University, Evanston, IL, USA.

[*]E-mail: igalsz@northwestern.edu

⊥ These two authors contributed equally

Abstract:

We develop and apply a molecular theory to study the adsorption of lysozyme on weak polyacid hydrogel films. The theory explicitly accounts for the conformation of the network, the structure of the proteins, the size and shape of all the molecular species, their interactions as well as the chemical equilibrium of each titratable unit of both the protein and the polymer network. The driving force for adsorption is the electrostatic attractions between the negatively charged network and the positively charged protein. The adsorption is a non-monotonic function of the solution pH, with a maximum in the region between pH 8 to 9 depending on the salt concentration of the solution. The non-monotonic adsorption is the result of increasing negative charge of the network with pH, while the positive charge of the protein decreases. At low pH the network is roughly electroneutral, while at sufficiently high pH the protein is negatively charged. Upon adsorption, the acid-base equilibrium of the different amino acids of the protein shifts in a nontrivial fashion that depends critically on the particular kind of residue and solution composition. Thus, the proteins regulate their charge and enhance adsorption in a wide range of conditions. In particular, adsorption is predicted above the protein isoelectric point where solution lysozyme and the polymer network are both negatively charged. This behavior occurs because the pH in the interior of the gel is significantly lower than in the bulk solution and it is also regulated by the adsorption of the protein in order to optimize protein-gel interactions. Under high pH conditions we predict that the protein changes its charge from negative in the solution to positive within the gel. The change occurs within a few nanometers at the interface of the hydrogel film. Our predictions

show the non-trivial interplay between acid-base equilibrium, physical interactions and molecular organization under nanoconfined conditions that leads to non-trivial adsorption behavior that is qualitatively different from what would be predicted from the state of the proteins in bulk solution.

1. Introduction

The rational design of novel materials for applications in a variety of bio-related fields, including tissue engineering,[1] biosensensing,[2] controlled protein-delivery,[3, 4] and protein separation using chromatography,[5] requires a profound understanding of the physical and chemical mechanisms that contribute to the adsorption of proteins on surfaces. Protein adsorption in hydrogels is a complex process that involves a variety of physical interactions including van der Waals, electrostatic, steric, together with the important entropic factors related to the distribution of counterions and coions as well as the conformational degrees of freedom of the polymer network. Moreover, the physical interactions are strongly coupled to the chemical state of both the protein and the gel. Consider for example electrostatic interactions that arise from the interactions between the charged amino-acids in the proteins with the charged gel monomers. The state of the charge of the different groups depends on the pH, solution ionic strength and very importantly on the local molecular organization. Namely, the acid-base equilibrium is strongly coupled to the molecular organization and physical interactions. As we demonstrate, this coupling leads to emergent behavior that results in non-trivial titration curves for the different amino-acids whose variation from bulk solution conditions depends on the location of the group within the protein sequence.

Ion exchange chromatography (IEC) is a separation method based on electrostatic interactions to separate globular proteins.[6] In cation exchange chromatography, for example, positively charged proteins ($pH < pI$) are attracted to a negatively charged solid supports (ion-exchange resins).[7, 8] The negative surface charge of the resin is initially neutralized by small cations, counterions, which later desorb as the proteins

adsorb. The load capacity of these resins compares to that of charged surfaces ($2-3\ mg/m^2$).[9] These resins can be modified using polymeric chains that form thin hydrogel films on the surface. If the polymer contains titratable groups, the proper choice of solution conditions can produce a significant enhancement in protein adsorption as compared to the bare surface.[10] The improvement in the load capacity occurs because the polyelectrolyte tethered to the surface offers the possibility of adsorption in three dimensions (or more appropriately in multilayers that span the thickness of the film) as opposed to the two-dimensional adsorption on charged bare surfaces. The molecular organization and charge state of these films depend critically on the conditions of the environment (solution pH, salt and protein concentration). Moreover, the state of charge of the protein depends on the composition of the surroundings. Consequently, the degree of adsorption, the three-dimensional distribution of adsorbed proteins and the preferential selectivity of different proteins by the resin are all critically coupled to the conditions of the medium. Thus, the rational design of applications that require optimal protein adsorption requires a deep understanding of the role of the environment on the adsorption of proteins on environment-sensitive polymer films.

Using calorimetry, Welsch *et al.*[11] studied lysozyme adsorption on negatively charged core-shell microgels at $pH = 7.2$ and ionic strength of $7-17\ mM$. This study shows that the protein gains approximately one positive charge (protonation) upon entering the hydrogel. Some questions naturally arise from this experiment and for the thorough understanding of IEC: which amino acids are responsible for this protonation? Where does this protonation occur, inside or outside the gel? How does the state of charge of the protein depend on the environment? Is this observation a generic result or is

it specific to this study? The answer to these questions requires a fundamental understanding of the process. In particular, it is necessary to describe the coupling that exists between acid-base equilibrium, the molecular organization and the interactions in these nanoconfined systems.

In this work, we present a systematic study of the adsorption of proteins on pH responsive hydrogels using a theory that allows for a molecular-level description of all the components in the system, including lysozyme and the polymer network. The molecular theory explicitly considers the conformational degrees of freedom of the polymer network, the structure of the protein, the size, shape and charge distribution in all molecular species as well as the acid-base equilibrium of all the titratable components of the system. Namely, the theory does not assume the state of protonation of each group but predicts it depending on the molecular organization and the optimal distribution that minimize the *total* free energy of the system. Thus, the theory enables systematic studies of the adsorption process while providing physical-chemical insights of the factors that determine the adsorption behavior as a function of the solution controllable variables. In particular, we will show the emergent behavior that arises due to the coupling between the molecular organization of the combined hydrogel-adsorbed protein, the physical interactions and the chemical state of titratable amino acids and gel segments.

There are several studies in the literature of protein adsorption on surfaces using molecular simulations.[12, 13] These works have generally focused on lysozyme[14-19] because it is a well characterized globular protein with a compact and very stable structure.[20, 21] Different approximations have been used to describe lysozyme, from full atomistic[15-18] to coarse-grained models.[14, 22] Although insightful information can be obtained from these

molecular simulations, they can generally only incorporate a few protein molecules. Modeling protein adsorption inside hydrogel films requires a considerable number of protein molecules. More appropriately, adsorption isotherms can only be determined if both the solution and the adsorbed proteins are explicitly considered. Moreover, the polymer network, small ions and solvent molecules, need to be also properly treated and therefore computer simulation become computationally intractable for the systematic studies of these systems. An important consideration in the adsorption is the treatment of the acid-base equilibrium of the different titratable species (protein residues, network segments, etc.) which can vary locally, due to spatial variation of the pH (given by the local concentration of protons), a daunting task for molecular dynamics simulations, even though some aspects of the effect of pH in the protonation of protein residues can be treated with Monte Carlo simulations in semigrand canonical ensemble.[23, 24]

Protein adsorption on charged surfaces and polyelectrolyte layers has been studied theoretically[25-29]. Biesheuvel and Wittemann[26] used a mean-field theory to investigate the adsorption of bovine serum albumin (BSA) on spherical weak polyelectrolyte brushes. They predicted adsorption even when the solution pH is above the isoelectric point of the protein. This behavior, according to their predictions, results from the fact that the brush pH is lower than the protein pI. Thus, the protein reverses its charge from negative to positive as it adsorbs. Similar results were predicted for the adsorption of BSA on planar poly(acrylic acid) layers using an analogous approach[27]. In line with these predictions, de Vos *et al.*[28] suggested that the main effect that allows adsorption above the pI is charge regulation by the protein, as opposed to an inhomogeneous charge distribution on the protein surface, as suggested by previous studies.[30] The two effects, however, can

contribute additively to the absorption above pI.[28] The theoretical studies that predict adsorption above pI incorporate charge regulation by both the polymer layer and the protein. However, the protein is modeled as a rigid geometric object (either a cylinder or a sphere) without detailed information of its three dimensional structure or the role that the distribution of titratable amino-acid on the protein play on the adsorption behavior.

The molecular theory we use in this work is an extension of the general approach developed to study responsive polymer gels[31, 32] and protein adsorption on surfaces with grafted polymers[33]. The predictions of this theory for the properties of polyacrylic acid layers as a function of pH and salt concentration[34] as well as the predictions for amount of adsorbed protein as a function of the surface coverage of polymer were shown to be in very good agreement with experimental observations. The proteins that were studied include lysozyme, fibrinogen and streptavidin in a variety of different modified surfaces including long and short PEG layers[35-37] and peptoid modified surfaces[38]. Very recently the theory was generalized and applied to study the adsorption of hexahistidine on polyacid hydrogel films.[39] The predicted adsorption of the pH-sensitive peptide depends critically on the solution salt concentration, and it shows a non-monotonic behavior as a function of the pH. Moreover, this previous study shows the importance of considering the coupling between all the contributions in describing the adsorption process. In the present work we extend the application of the theory to the adsorption of the more complex lysozyme. We will show how we obtain qualitative different results from the polypeptide adsorption as the different acid and basic amino acids show response to pH that depends exquisitely on the type of group and its distribution within the protein. Moreover, the response of the film to the adsorption of the protein is very different from

that of the polypeptide, demonstrating the importance of molecular details in the adsorption behavior as well as providing a tool for the guidance of experimental systems to obtain protein adsorption.

2. Methods

Consider a polyacid network, e.g. polyacrylic acid gel, chemically grafted to a substrate surface defined by the plane $z = 0$ (see Figure 1). The coordinate z measures the distance from the supporting planar surface of total area A. The number of grafting points of the polymer network to the surface is denoted by σ. The weak polyelectrolyte network is in contact with a solution containing water molecules (w), protons (H^+), hydroxyl ions (OH^-), and monovalent salt ($NaCl$) completely dissociated into sodium cations (Na^+) and chlorine anions (Cl^-). The solution contains lysozyme at concentration c_{Lys}^{Bulk}.

To study the thermodynamics of lysozyme adsorption on the pH-sensitive hydrogel film, we employ a theory that explicitly includes the size, shape, charge distribution and conformations of all molecular components, including the polymer network and the protein. Furthermore, the molecular theory predicts the protonation state of the acid and basic groups depending on their position and local environment. Namely, the chemical state is coupled with the conformational degrees of freedom of the polymer network, the electrostatic, van der Waals and excluded volume interactions, as well as the entropy loss of solvent and ion confinement. This is done through the formulation of a general free energy that explicitly includes the coupling between the chemical state, molecular organization and physical interactions. The details of the theory were recently

presented and used to study the adsorption of hexahistidine (his-tag) within the same kind of pH-sensitive adsorbent materials[39].

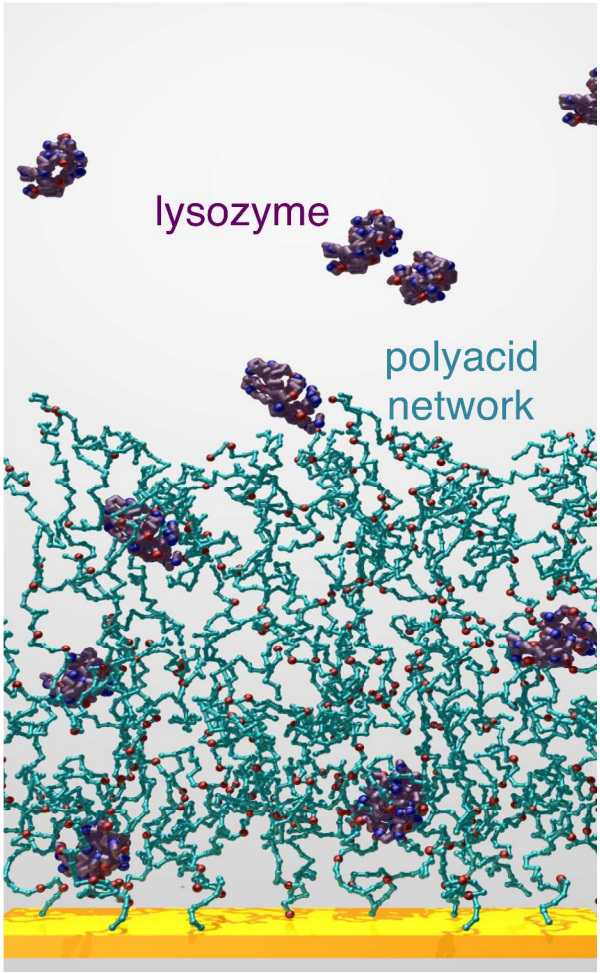

Figure 1. Schematic representation of the hydrogel thin film in contact with a protein solution: a polyacid network (green lines), chemically grafted to a planar solid surface, in equilibrium with a salt solution that contains lysozyme at concentration c_{Lys}^{Bulk}. The bulk composition of the solution (*i.e.*, its pH, c_{salt} and c_{Lys}^{Bulk}) is externally controlled. Red spheres in the network and in the protein represent negatively charged units, while blue spheres in the protein denote positively charged residues.

The first step in this theoretical approach consists in writing all the different contributions to the total Helmholtz free energy of the system:

$$F = -TS_{ConfN} + F_{ChmN} - TS_{Mix} - TS_{TR} + F_{ChmP} + U_{Elect} \qquad (1)$$

where T is the temperature, S_{ConfN} is the conformational entropy of the polymer network of the hydrogel film, F_{ChmN} represents the chemical free energy that described the acid-base equilibrium of the network, S_{Mix} is the mixing (translational) entropy of the (small) mobile species (w, H^+, OH^-, Na^+ and Cl^-). S_{TR} represents the translational and rotational degrees of freedom of the protein. F_{ChmP} is the protein chemical free energy, which accounts for the acid-base equilibrium of the titratable residues of lysozyme molecules. U_{Elect} represents the total electrostatic energy of the system. In this work we are not explicitly accounting for different hydrophobic (or van der Walls) interactions between the polymer network and the different amino-acids. This has been shown to be a very good approximation for lysozyme[36]. Moreover, we want to emphasize the interplay between acid-base equilibrium, electrostatic interactions and molecular organization of the film.

Each of the contributions to the free energy are expressed as functionals of: 1) the probability of the different molecular conformations of the network, 2) the position-dependent (local) probability of the different orientations of the protein, 3) the local density profiles of the protein, 4) the density profiles of the other mobile species, 5) the local degree of protonation of network segments and that of all titratable residues of the protein, and 6) the local electrostatic potential. We build a semi-grand potential, as the Legendre transform of the Helmholtz free energy, to account for the constant chemical

potentials of all the mobile species, i.e. that the thin film is in contact with a solution of proteins and ions. The extremum of the semi-grand thermodynamic potential, subject to packing constraints that model the intermolecular repulsive interactions and the constraint of global electroneutrality, provides explicit expressions for all the densities, the local protonation states and probabilities in terms of the position dependent electrostatic and repulsive interaction fields. These interaction fields are calculated by numerically solving the incompressibility constraint and the Poisson equation. Once the interaction fields are determined, the free energy of the system can be calculated. Thus, any thermodynamic quantity of interest can be computed by taking the proper derivative of the appropriate thermodynamic potential. Furthermore, all structural properties can be calculated from the interaction fields, the probabilities of network and protein conformations.

The numerical solution of the equations derived from the theory requires the definition of molecular models to describe all the species. In particular, the set of molecular conformations of the polymer network is an input of the theory. These conformations are obtained using molecular dynamics (MD) simulations. The network is composed of 25 segment-long chains inter-connected at six-coordinated crosslinking segments. Most of these chains connect two crosslinks, apart from the topmost chains that have their solution-side ends free, and some chains that are grafted by one of their ends to fixed positions on the surface. Grafting points are arranged on the surface forming a square lattice, with grafting density σ. The intrinsic logarithmic acidity constant of a network segment is taken as $pK_N = 5$ to represent a carboxylic acid such as acrylic acid. More detailed information on the molecular model used to describe the polymer backbone and on the MD simulations is presented in the SI and elsewhere.[32]

Lysozyme is represented by a coarse-grained model where the atoms of each amino acid are knit together in a single bead located at the position of the corresponding α-carbon. The position of all atoms is obtained from the crystallographic structure PDB file (193L).[20] The positions of all the beads, relative to the center of mass of the molecule, are maintained fixed according to the original PDB conformation. The molecule as a whole, however, has rotational and translational degrees of freedom. The amino acid residues are classified in two kinds, *neutral* and *titratable*. The titratable residues include aspartic (Asp), glutamic (Glu), tyrosine (Tyr), arginine (Arg), histidine (His) and lysine (Lys). Each of these residues is characterized by an intrinsic acidic constant (Ka_{aa} with $aa \in \{Arg, His, Lis, Asp, Glu, Tyr\}$). Table 1 shows the values of the different intrinsic pKa used in this work,[40, 41] as well as the composition number cn_{aa} that gives the number residues of each kind that form the molecule. The rest of amino acids are defined as neutral segments. Cysteine, in its free form is a titratable amino acid. Lysozyme has 8 cysteine residues, but they form 4 bridge bonds. Thus, these residues cannot ionize, and hence are included in the neutral group. As we will show the acid-base equilibrium when the protein adsorbs in the gel is very different from that of the bulk solution.

A more detailed description of the theory, the equations solved and the input molecular models and conformations for protein, gel and ions is presented in the SI, see also [39].

	Asp	*Glu*	*Tyr*	*Arg*	*His*	*Lys*	*Neutral*
cn_{aa}	7	2	3	11	1	6	99
pKa	4.0	4.4	9.6	12.0	6.3	10.4	

Table 1. Composition number cn_{aa} and the intrinsic pKa of all the different amino-acids included in the coarse-grained model of lysozyme.

3. Results and Discussion

We study the adsorption of lysozyme on model polyacrilic acid gel. The minimization of the total free energy of the thin film gel in contact with a protein solution for a given solution condition, i.e. pH, salt and protein concentrations, provides the local molar concentration of all the molecular species as well as the molecular organization of the hydrogel film. Namely, the concentration profiles of all the species is the one that results from having the chemical potential of each species equal everywhere within the film up to the bulk solution. The adsorption is defined as

$$\Gamma = M_{Lys} \int_{z=0}^{z=\infty} \left(c_{Lys}(z) - c_{Lys}^{Bulk} \right) dz, \qquad (2)$$

where M_{Lys} is the molar mass of lysozyme and $c_{Lys}(z)$ is the position dependent lysozyme concentration. Thus, the adsorption gives the total mass excess per unit area of lysozyme located inside the film and in the interfacial region. Local profiles of lysozyme concentration under different conditions of pH and salt concentration are presented in the Supporting Information (SI).

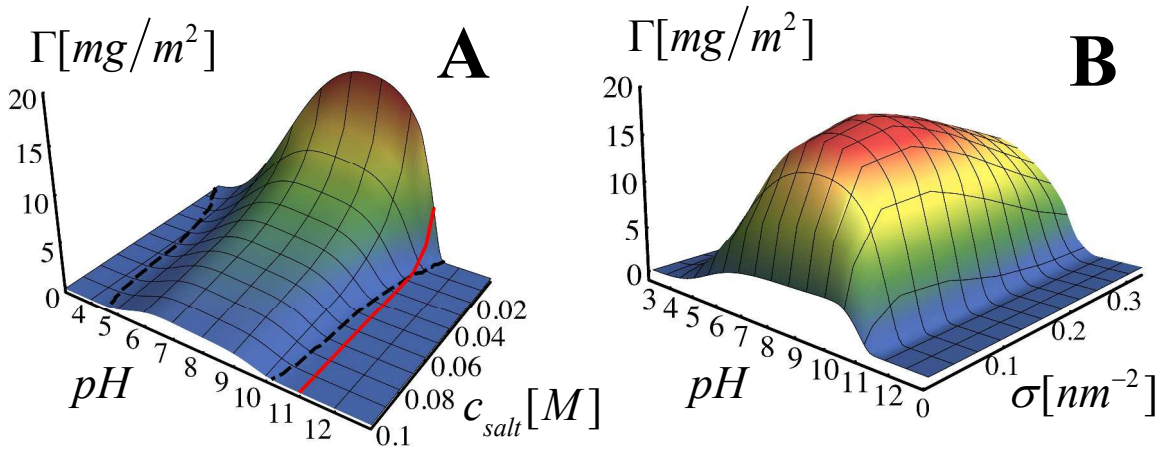

Figure 2. A) Protein adsorption, Γ, as a function of the solution pH and salt concentration, c_{salt}, for a network with grafting density, $\sigma = 0.084\ nm^{-2}$. The red line is a constant-pH curve on the surface that gives the isoelectric point of lysozyme in the bulk solution, $pI = 10.9$. Both black dashed lines correspond to $\Gamma = 0$. The adsorption is positive within the region delimited by those lines and negative (depletion) outside. B) Protein adsorption, Γ, as a function of pH and gel grafting density, σ, for $c_{salt} = 10^{-3}M$. In both panels, the bulk concentration of protein is $c_{Lys}^{Bulk} = 10^{-4}M$.

Figure 2A shows the adsorption of lysozyme as a function of the solution pH and salt concentration. For a given pH, the adsorption increases monotonically as the salt concentration decreases. This result is a signature that the driving force for adsorption is the electrostatic attractions between the negatively charged network and the positively charged amino acids. At high salt concentration, protein-network attractions are screened by the presence of significant amounts of monovalent salt ions. Such screening weakens as the salt concentration decreases, allowing the amount of adsorbed protein to increase.

The dependence of Γ on the solution pH is non-monotonic, Figure 2A. For highly acidic or basic pH values, the adsorption is negligible. At low pH, the protein has a large positive charge (see Figure 4A), however only a small fraction of the network titratable groups are ionized. At sufficiently high pH, the backbone of the gel is significantly charged, but the net charge of the protein is also negative. At intermediate pH values Γ

can be large, depending on the salt concentration. The network is strongly (negatively) charged and the net charge of lysozyme is positive. (A more quantitative description of the state of charge of both the protein and the network is given below). The adsorption shows maxima that can reach up to nearly $18\,mg/m^2$ for the lowest salt concentration considered. This adsorption is sixfold the value reported in experiments of lysozyme interacting with charged bare surfaces.[9] Thus, we clearly see the enhancing role that the pH-sensitive film has on the adsorption of the protein due to the addition of a nanometric third dimension where lysozyme adsorbs on the film.

The black dashed lines in Figure 2A give the condition $\Gamma = 0$, which separates the adsorption region ($\Gamma > 0$) from the two regions where depletion ($\Gamma < 0$) is predicted. The range of pH values where adsorption occurs, enclosed by such lines, widens as the salt concentration decreases. In the same panel of Figure 2, a constant-pH curve on the Γ surface (solid red line) illustrates the solution isoelectric point of lysozyme, pI. In the bulk solution, the net charge of lysozyme is positive if $pH < pI$, negative if $pH > pI$, and exactly zero when $pH = pI$. Therefore, from solution considerations, no adsorption is expected if the pH is above the isoelectric point of the protein. At low c_{salt}, however, there is appreciable lysozyme adsorption for pH values above pI. We show below that this is due to the change in the charge of the protein when adsorbed within the gel.

The effect of grafting density of the network on the adsorption is shown in panel B of Figure 2, for a relatively low salt concentration ($c_{salt} = 10^{-3}M$). The dependence of Γ on the pH is qualitatively similar for different grafting densities. Namely, the adsorption shows the same non-monotonic behavior described in Figure 2A. However, the magnitude of the adsorption depends critically on the grafting density of the polymer

network. There is an intermediate σ that maximizes the amount of adsorbed lysozyme. As σ increases, so does the density of ionizable units of the network, which can enhance the ability of the lysozyme to adsorb due to the electrostatic attractions with the hydrogel. However, two other effects have to be considered. First, at a given pH, a higher density of polymer results in a lower degree of charge in the hydrogel backbone due to intra-network electrostatic repulsions.[42] Second, if the density of polymer is high enough steric repulsion between the polymer segments and the protein tends to reduce the penetration of protein inside the hydrogel. Indeed, the predictions of Figure 2B indicate that the maximum of Γ occurs at a grafting density, $\sigma \approx 0.11\, nm^{-2}$, which corresponds to an average pore size of approximately $3.0\, nm$ in diameter. This value is similar to the diameter of the protein $d_{lysozyme} \sim 2.8\, nm$ (calculated as twice the radius of gyration of the crystallographic structure). Thus, we predict that the maximum adsorption is obtained when the pore size is commensurate with the protein size, which suggests that the steric effect is the most important limiting factor for the adsorption under these conditions.

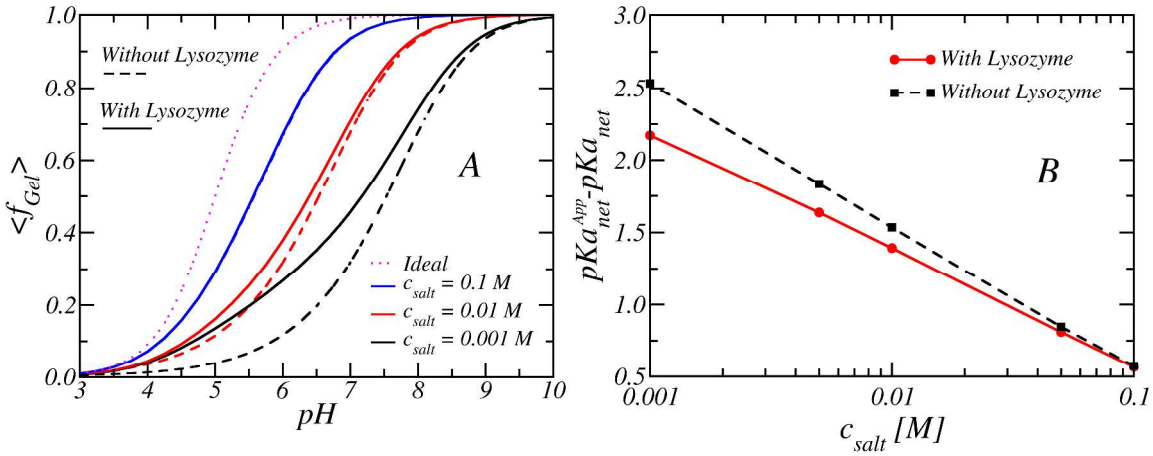

Figure 3. A) The average degree of dissociation of network units, $\langle f_{Gel} \rangle$, as a function of pH, for different salt concentrations. Solid lines correspond to the case in the presence of lysozyme in solutions while the dashed lines are in the absence of proteins. The magenta dotted line corresponds to the ideal titration curve of the monomer. B) Difference between the apparent and intrinsic pKa of network segments, pKa_{net}^{App} and pKa_{net}, as a function of the salt concentration, c_{salt}. In both panels, the network grafting density is $\sigma = 0.084\, nm^{-2}$, and when the solution contains lysozyme, its concentration is $c_{Lys}^{Bulk} = 10^{-4} M$.

Next, we study in detail the charging behavior of the polymer network and the adsorbed protein. The goal is to determine the mechanisms that underlay the non-monotonic pH-dependent adsorption, as well as to understand the adsorption predicted above the solution protein pI. Namely, we address how the acid-base equilibrium is different within the polymer gel as compared to the bulk solution. The ionization of the polymer network is quantified using the weighted average degree of dissociation

$$\langle f_{Gel} \rangle = \frac{\int_0^\infty f_{Gel}(z) \langle \phi_{Pol}(z) \rangle dz}{\int_0^\infty \langle \phi_{Pol}(z) \rangle dz}, \qquad (3)$$

where $\langle \phi_{Pol}(z) \rangle$ is the local volume fraction of network polymer and $f_{Gel}(z)$ is the local degree of dissociation. The angle brackets represent an ensemble average over the conformations of the polymer network. The average degree of charge measures the fraction of all the titratable units of the network that are deprotonated (charged). Figure

3A shows $\langle f_{Gel} \rangle$ as a function of the solution pH for various salt concentrations, both in the presence and absence of adsorbed lysozyme. In both cases, the ionization profiles are displaced to higher pH values respect to the ideal solution dissociation given by the intrinsic pKa of these acid groups, $pKa_{net} = 5$. The shifts occur because as the pH increases, so does the number of charged segments. Therefore, the increasing intra-network electrostatic repulsions disfavor the presence of negative charge, shifting the chemical equilibrium towards the protonated (uncharged) species. The shift in acid-base equilibrium comes at the price of increasing the chemical free energy, however, this is less costly than the electrostatic repulsions.[31]

Figure 3A shows that in the absence of lysozyme, the shift in $\langle f_{Gel} \rangle$ from the ideal behavior is larger than in the presence of the proteins, particularly at low pH and c_{salt}. As the solution pH increases, the hydrogel adsorbs salt ions, which screen the intra-network repulsions and neutralize the total electric charge of the film. The range of the electrostatic repulsions decreases as the concentration of ions grows, as would be expected due to the decrease of the Debye length. At low c_{salt}, there is a very high entropy loss of confining counterions, therefore the screening of the electrostatic interactions is weak. Then, the network prefers to shift the acid-base equilibrium to reduce the charge, paying the price of increasing the chemical free energy by reducing the price of electrostatic repulsions and counterion confinement. At high c_{salt}, on the other hand, significant concentrations of both positive and Cl^- ions are found inside the film. The larger screening of the electrostatic interactions allows for more dissociation in the network to relax the chemical free energy. Thus, the displacement of the dissociation curve is more significant as c_{salt} decreases. It is important to emphasize that this effect

shows the dual (and opposite) role of the salt concentration: increasing screening results in an increase charge.[43]

The presence of lysozyme in the solution results in competing adsorption between proteins and small cations. In general, competitive adsorption depends on two major factors: the concentrations of the competing species in the bulk solution, and their physical properties including molecular volume and electric charge. Namely, the competitive adsorption depends on the interplay between the ideal (concentration) and non-ideal (interactions) contributions to the chemical potential. In particular, the net charge of lysozyme is a critical factor, since adsorption of a single protein results in the release of as many small counterions as the net charge of the protein. The balance in the gain by the counterion release must be larger than the repulsive interactions arising from the larger size of the adsorbed proteins.

In the range of moderate to high salt concentrations ($c_{salt} > 0.01M$), there is weak protein adsorption. Thus, the pH-driven ionization of the network is quantitatively similar with and without the protein (Figure 3A). At lower salt concentrations, however, the adsorption of lysozyme leads to an increase of the network's degree of charge, as compared to the solution without the proteins. This behavior is more pronounced as the salt concentration decreases. Under these conditions, the solution concentration of protein is orders of magnitude lower than that of salt cations. In addition, a lysozyme molecule is significantly larger than a Na^+ ion. Both factors (size and concentration) favor the adsorption of small cations. However, lysozyme bears several positive charges, making the adsorption of protein a more effective mechanism for shielding the negative charge of network segments, with only the entropic cost of confining one particle as opposed to

several positive charges. Moreover, the shift in the titration curves of the hydrogels in the presence of the proteins is towards that of the ideal case, resulting in a lower chemical free energy cost for the network. The balance of all these contributions leads to more protein adsorption as the solution salt concentration decreases.

The ionization of the polymer network can be further characterized using the apparent pKa of the hydrogel, pKa_{net}^{App}, which gives the solution pH at which half of the titratable units of the network are charged. For the isolated acid group in a dilute solution (ideal solution) the transition midpoint is given by the intrinsic pKa. Figure 3B displays the difference between the apparent and the intrinsic pKa as a function of the salt concentration for solutions with and without lysozyme. In both cases, the apparent pKa of the gel moves towards the intrinsic value (*i.e.,* $pKa_{net}^{App} - pKa_{net}$ approaches zero) as the salt concentration increases. This behavior is due to the increasing adsorption of salt ions with c_{salt}, which results in a stronger screening of the intra-network electrostatic repulsions that favors dissociation. At high c_{salt}, lysozyme adsorption is negligible and the apparent pKa of the network is the same for both solutions. At low salt concentration, however, pKa_{net}^{App} can be more than two units higher than the intrinsic value. The screening of the electrostatic repulsions between charged segments is weak, disfavoring the dissociation of charge in the network. As already discussed, lysozyme can screen the electrostatic repulsions more efficiently because it offers more charge at less confinement cost and as a result the pKa_{net}^{App} is lower for lysozyme solutions.

It is important to emphasize that in nanoconfined systems, like the ones studied here, the pKa is not enough to characterize the titration curves, as it is in the ideal solution case. The reason is that, as clearly observed in figure 3A, the width of the

titration curve is much broader than the ideal case, and furthermore the titrations are not symmetric.

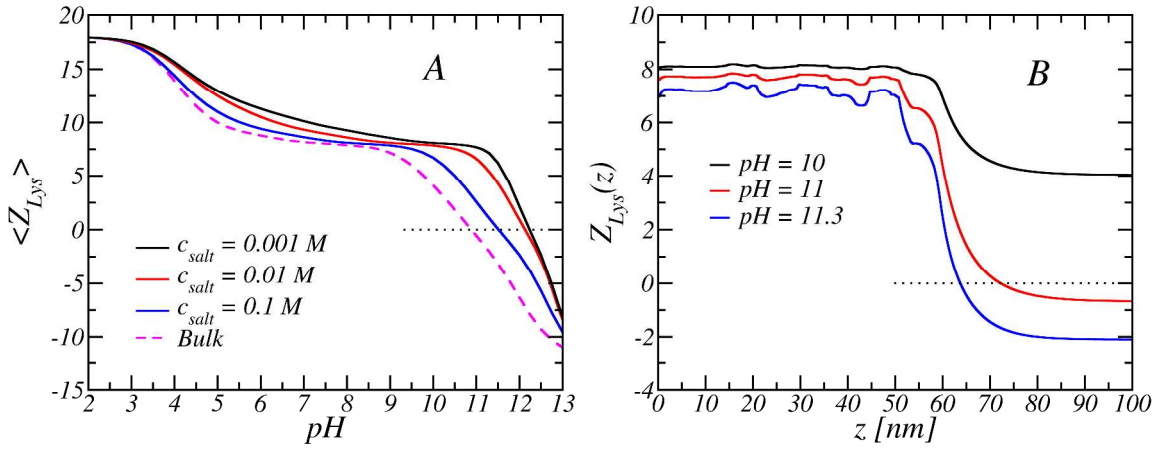

Figure 4. A) The average net charge of lysozyme inside the hydrogel film, $\langle Z_{Lys} \rangle$, as a function of the pH for different salt concentrations (solid lines). The magenta dashed line represents the charge of the protein in the bulk solution, Z_{Lys}^{Bulk}. B) The local net charge of the protein, $Z_{Lys}(z)$, as a function of the distance from the surface, z, for different solution pH values and $c_{salt} = 10^{-3}M$. In both panels, the bulk concentration of lysozyme is $c_{Lys}^{Bulk} = 10^{-4}M$, and the network grafting density is $\sigma = 0.084\, nm^{-2}$. Dotted lines give the conditions $\langle Z_{Lys} \rangle = 0$ and $Z_{Lys}(z) = 0$ in panels A and B, respectively.

The next question that we address is how the adsorption of the proteins changes their charges. To this end, it is convenient to define the average net charge of the protein inside the film as

$$\langle Z_{Lys} \rangle = \frac{\int_{z=0}^{z=H_{Gel}} Z_{Lys}(z) dz}{H_{Gel}}, \qquad (4)$$

where $Z_{Lys}(z)$ is the local charge of the protein at a distance z from the supporting surface, which is given by the contributions of the local charge of the titratable residues belonging to molecules with center of mass at z. H_{Gel} is the network thickness, defined as

$$H_{Gel} = \frac{\int_0^\infty (2z)\langle\phi_{Pol}(z)\rangle dz}{\int_0^\infty \langle\phi_{Pol}(z)\rangle dz}, \qquad (5)$$

Figure 4A shows $\langle Z_{Lys}\rangle$ as a function of the pH for different salt concentrations. The net charge of the protein in the bulk solution, Z_{Lys}^{Bulk}, is also shown in the figure. Under strong acidic conditions, both adsorbed and bulk proteins have a positive electric charge that is the maximum possible considering the total number of basic residues (Arg, His and Lis) that compose the lysozyme molecule (see Table 1). As the solution pH increases, Z_{Lys}^{Bulk} and $\langle Z_{Lys}\rangle$ drop rapidly, and at intermediate$-pH$ there is a region with a small slope (plateau-like), followed by a sharp decrease towards negative charge at high pH. In bulk solutions the plateau like region extend from pH 6 to 9, and in this range Z_{Lys}^{Bulk} decreases less than two unit charges. For the adsorbed proteins, the positive charge and the range of pH where this region is observed to depend on c_{Salt}.

In bulk solution, the calculated isoelectric point of lysozyme is, $pI \approx 10.9$, in agreement with the value experimentally reported.[44] Adsorbed proteins, however, can remain positively charged more than one or two units of pH above the solution pI, depending on the salt concentration. The apparent isoelectric point of adsorbed lysozyme, pI_{App}, defined as the pH at which $\langle Z_{Lys}\rangle = 0$, is higher than pI for all c_{Salt}, and it increases with decreasing salt concentration.

The net charge of adsorbed lysozyme is always larger than the bulk value, $\langle Z_{Lys}\rangle > Z_{Lys}^{Bulk}$, for all solution compositions, as shown in Figure 4A. This implies that the negative charge of the hydrogel network induces a shift in the titration curves of the protein amino acids. This behavior occurs to favor the adsorption of the protein within the film, and thus releasing counterion to the solution. This is a particular large effect at

low salt concentrations when the range and strength of the electrostatic interactions is large. Therefore, at low c_{Salt} $\langle Z_{Lys}\rangle$ shows a larger deviation from Z_{Lys}^{Bulk} and there is significant adsorption (Figure 2A). For $pH > pI_{App}$, the adsorbed proteins are negatively charged and as a result depletion ($\Gamma < 0$) is predicted (Figure 2A).

One interesting feature of Figure 4A is that for a given salt concentration, there is a range of pH values where the protein is negatively charged in the bulk solution but positively charged inside the film. This implies that as the protein approaches the film, its charge reverses sign. Figure 4B shows the local charge of the proteins as a function of the distance from the surface. Three different regions can be clearly distinguished. Inside the film ($z < H_{Gel}$~$50\ nm$), the charge of the protein shows only small fluctuations around its average adsorbed value $\langle Z_{Lys}\rangle$. The small fluctuations in charge inside the film are a manifestation of the local structure of the network. Far from the surface ($z > 75\ nm$), the charge of lysozyme is that of the bulk solution, Z_{Lys}^{Bulk}. The third region is the interface between the film and the bulk solution, where the local charge of the protein goes from Z_{Lys}^{Bulk} to $\langle Z_{Lys}\rangle$ as z decreases.

In the interfacial region, which spans no more than $20\ nm$ (about the size of the Debye length for this salt concentration) the charge of the protein can increase several units as the molecule adsorbs. This increase is more significant when the bulk charge is negative and the protein charge reverses. In particular, at $pH = 11.3$, the charge of the protein is roughly $-2e$ in bulk solution and it increases up to $+7e$ when adsorbed inside the hydrogel. Under such solution conditions, lysozyme adsorption is still significant (see Figure 1A and SI), although the hydrogel and the solution protein have the same negative charge. This result shows the importance of considering the combined hydrogel-protein

system in describing the adsorption due to the local nature of acid-base equilibrium. Moreover, it shows the important qualitatively wrong conclusions that can be achieved by predicting the behavior of responsive nanoconfined systems from bulk solution considerations.

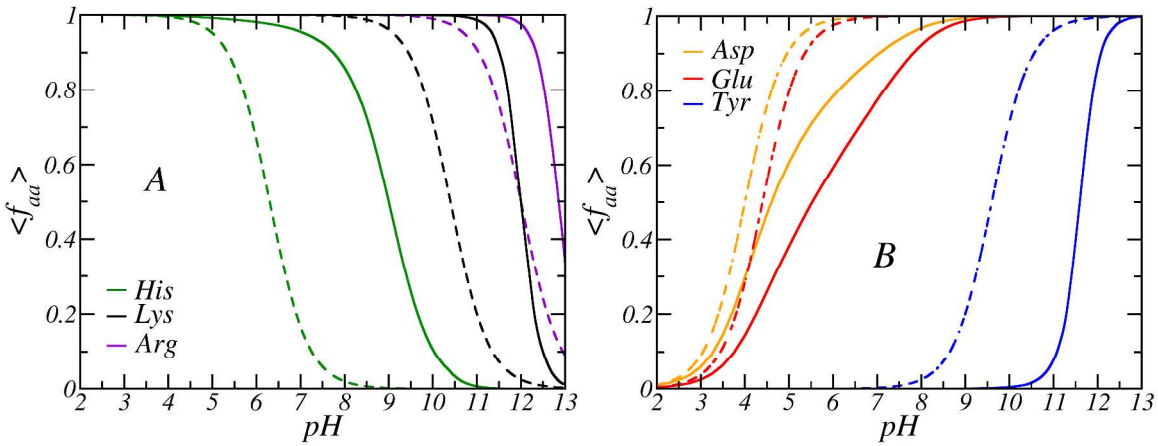

Figure 5. The fraction of protonated basic (a) and deprotonated acidic (b) residues of adsorbed proteins (solid lines) as a function of the pH. The solution concentrations of salt and protein are $c_{salt} = 10^{-3}M$ and $c_{Lys}^{Bulk} = 10^{-4}M$, respectively. The network grafting density is $\sigma = 0.084\, nm^{-2}$. Dashed lines give the degree of charge of the amino acid in the bulk solution.

We have shown that the charge of lysozyme changes significantly due to adsorption. The question we address now is how each of the individual amino acids within the protein responds to the local environment within the gel. For adsorbed molecules, the average degree of charge of a particular residue is defined as

$$\langle f_{aa} \rangle = \frac{\int_{z=0}^{z=H_{Gel}} f_{aa}(z)\langle \phi_{aa}(z) \rangle dz}{\int_{z=0}^{z=H} \langle \phi_{aa}(z) \rangle dz} \text{ with } aa \in \{Arg, His, Lis, Asp, Glu, Tyr\}, \quad (6)$$

where $f_{aa}(z)$ and $\langle \phi_{aa}(z) \rangle$ are the local degree of charge and volume fraction of the amino acid. For a protein in bulk solution, the protonation state of its residues is described by the ideal solution titration curve defined by the intrinsic pKa of the acid (or conjugated acid for bases), pKa_{aa}, i.e. $f_{aa,bulk} = 1/\left(1+10^{pK_{aa}-pH}\right)$. Figure 5 shows the

degree of charge of basic (panel A) and acidic (panel B) residues in the case of adsorbed lysozyme (full lines) and bulk (dashed lines).

The protonation of basic residues (Arg, His and Lys) of adsorbed proteins is shifted towards higher values of pH to increase the positive charge of the molecule (see Figure 5A). The larger predicted shift at this low salt concentration ($c_{salt} = 10^{-3}M$) occurs for histidine, whose intrinsic pKa is in the pH region where there is significant adsorption, Figure 1. Each lysozyme molecule has only one His residue, which remains charged even at strong alkaline conditions when the protein is inside the hydrogel. The protonation of lysine residues also shifts significantly. Indeed, all six Lys units of adsorbed lysozyme remain positively charged in most of the pH range. The same is true for arginine residues although the shift is less significant, since the eleven Arg residues are mostly charged, even in the bulk solution.

It is important to emphasize that while all the basic groups shift their titration curve towards higher alkaline values they do it in very different ways. Namely, the titrations curves are not simply shifted with respect to their respective bulk values, but the width of the titration changes significantly. For His the titration within the gel is broader than the ideal case while for both Lys and Arg they are narrower. The reason for the difference in width is the result of the interplay between the electrostatic gain associated with shifting the overall charge of the proteins in the different regimes and the chemical free energy cost carried out by the shift from the ideal case.

Panel B of Figure 5 shows the dissociation of acidic residues as a function of the pH. To reduce the negative charge of the adsorbed protein, all the acidic residues are less charged than in the bulk solution at all pH values. The displacement in the dissociation

curves of aspartic and glutamic acid is smaller than that observed for tyrosine residues. However, the shape of the titration curves changes more significantly for Asp and Glu than for Tyr. This behavior is because bulk Asp and Glu residues are already strongly charged in the region where there is sufficient charge in the network to drive lysozyme adsorption. The intrinsic pKa of these amino acids ($pKa_{Asp} = 4$ and $pKa_{Glu} = 4.4$) is below that of the network segment ($pKa_{net} = 5$). On the other hand, $pKa_{Tyr} = 9.6$, but inside the film the three of Tyr residues remain mostly neutral up to pH 11.

With the information provided in both panels of Figure 5, we can now identify which residues are involved in the charge reversal upon adsorption, observed in Figure 4. When $pH = 11.3$ in Figure 4B, the protein gains 9 protons when going from the bulk solution to the interior of the hydrogel film, reversing the sign of its net charge from $\langle Z_{Lys} \rangle = -2$ to $+7$. The residues that play a key role in this behavior are Lys and Tyr. At $pH = 11.3$, Lys is fully protonated inside the film but weakly charged in the bulk solution (see Figure 5A). Likewise, Tyr is charged in the bulk solution but protonated for adsorbed lysozyme. Each lysozyme molecule has six and three of these residues, respectively, accounting for the nine positive charges gained during adsorption.

Experimental observations of lysozyme adsorption on a negatively charged core-shell microgel at $pH = 7.2$ and ionic strength of $7 - 17\ mM$ indicate that the protein gains approximately one positive charge upon entering the gel.[11] The predictions presented in Figure 5 are in agreement with these experimental findings. Moreover, our results suggest that under these conditions, the observed behavior is due to the protonation of the His residue when lysozyme adsorbs inside the polyacid network.

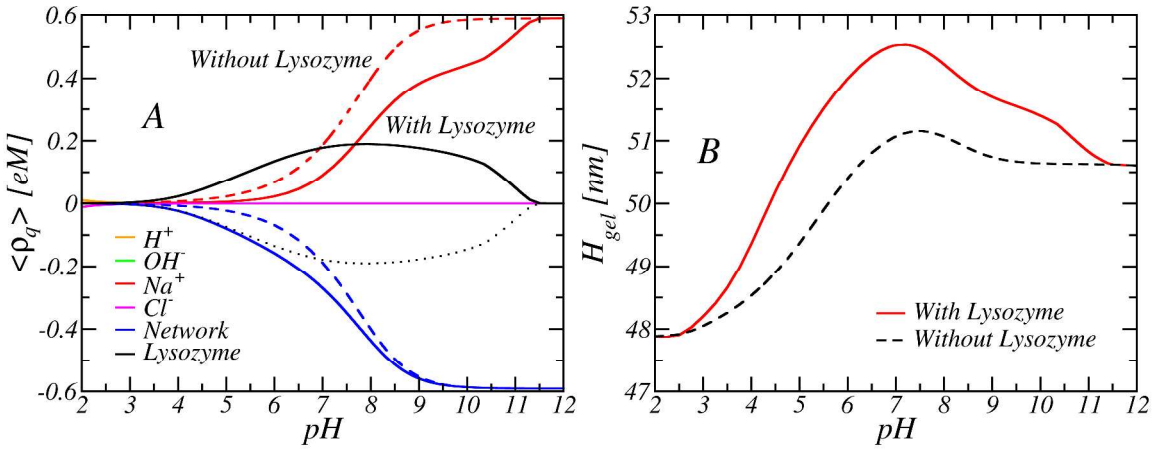

Figure 6. A) Average charge density of each species inside the film as a function of solution pH. B) The thickness of the film, H_{Gel}, as a function of the solution pH. In both panels, solid lines correspond to solutions with lysozyme concentration $c_{Lys}^{Bulk} = 10^{-4}M$, while dashed lines denote solutions without protein. The black dotted line in panel A) is a negative projection of the density of charge of lysozyme. In all the cases, $c_{salt} = 10^{-3}M$, and the network grafting density $\sigma = 0.084\ nm^{-2}$.

The proper treatment of the thin film with adsorbed proteins in contact with the solution requires that the system should be globally electro neutral. Namely, the total charges in the whole system should add up to zero. Interestingly, while we do not impose it, we obtain that in most (if not all) cases studied the total charge in film (from $z = 0$ to $z = H_{Gel}$) is roughly zero. In other words, the conditions that minimize the free energy under the constraint of global electroneutrality are such that the film is (almost) electroneutral. We can then analyze what are the different molecular species that contribute to the charge in the film. Figure 6A shows the average charge in the film arising from each molecular species as a function of the pH. The figure also includes the case for salt solutions without the protein. For low c_{salt} solutions without lysozyme, the network charge is neutralized exclusively by sodium cations, as can be seen since the

network charge and Na^+ profiles are a reflection of each other over the neutral charge value. We have chosen a low salt concentration in Figure 6. At higher c_{salt}, Cl^- ions will also adsorb inside the film, which carries with it the adsorption of additional cations (results not shown). For the case of lysozyme in the solution there is a higher density of charge in the polymer network at low and intermediate pH values and at low c_{salt}, as seen in Figure 6A (see also Figure 3). For $pH < 6$, the net positive charges of lysozyme molecules are the main (if not only) contribution that neutralize the negative charge of the network. Each protein bears several positive charges (see Figure 4A). The adsorption of fewer highly charged particles offers the same electrostatic gain as the equivalent number of small cations but without the entropic cost of confining the smaller Na^+. As the pH increases, the charge per protein decreases and while the number of adsorbed proteins continues to increase, the change in charge of the network cannot be completely neutralize by the protein due to the large steric repulsions involved in adding too many proteins. Therefore, sodium cations are needed in order to balance the negative charge of the network. At $pH = 7.8$, the protein and the small cation contribute the same number of positive charges to the interior of the film. This corresponds roughly to the maximum adsorption of proteins shown in Figure 1. At even higher pH's, the decrease in the charge of the protein results in smaller numbers of adsorbed proteins and an increase in the number of counterions needed to neutralize the continuously increasing charge of the film with pH.

The charging of the polymer backbone with pH leads to swelling of the thin film in order to increase the effective distance between charged units. For a hydrogel grafted to the supporting surface the only direction possible for swelling is the one perpendicular

to the surface. Thus, swelling of the film is fully characterized by its thickness H_{Gel}, calculated using equation 5. Figure 6B shows the film thickness a function of the pH in the presence and absence of adsorbed proteins. The swelling of the thin film has already been analyzed in previous work[32] and we show it here, to demonstrate the role that adsorption plays in the pH dependent swelling.

For lysozyme solutions, the non-monotonic swelling (swelling-deswelling) with increasing pH is more prominent than for salt solutions, as seen in Figure 6B. The reason for this behavior is the large volume occupied by the adsorbed proteins acting as the neutralizing agent compared to that of small cations. Interestingly, we have shown in previous work that the adsorption of polyhistidine leads to a shrinking of the thin film. However, the results presented in figure 6B shows the important role played by the size of the protein that results in chain stretching to accommodate the lysozyme within the network.

4. Conclusions

We have used a molecular theory to study the adsorption of lysozyme within a polyacid hydrogel film of nanometric thickness. The theory allows for a molecular-level description of all the components of the system, and it explicitly incorporate the coupling that exists between molecular organization, physical interactions and chemical equilibrium under nanoconfined conditions.

The main driving force for lysozyme adsorption is the electrostatic attractions between the negatively charged network and the positively charged protein. Thus, the adsorption of lysozyme depends critically on the composition of the bath solution that is

in equilibrium with the film. At very acid or alkaline conditions, depletion of lysozyme or negligible adsorption is predicted because either the network is weakly ionized (low pH) or the protein is negatively charged (high pH), respectively. The adsorption behavior is qualitatively similar for different salt concentrations, but lowering the salt content of the bath solution highly enhances adsorption.

The adsorption of lysozyme leads to a larger deprotonation of the network as compared to the absence of proteins. Moreover, the net charge of the adsorbed lysozyme is more positive than that of bulk solution proteins. In solution, the protein is negatively charged above its isoelectric point, pI. Thus, no adsorption is $a\ priori$ expected when $pH > pI$. However, the acid-base equilibrium for both protein and hydrogel shift significantly to optimize adsorption. Thus, adsorbed lysozyme is positively charged up to more than one unit above the solution pI. Depending on the experimental conditions, we predict that the protein can gain up to nine protons and reverse its charge upon adsorption. This dramatic charge reversal, from the solution to the film, occurs within a few tens of nanometers that represent the double layer formed at the interface of the thin film and the solution.

The molecular theory enables us to identify what residues are responsible for the protonation that lysozyme undergoes upon entering the film. Calorimetric evidence of lysozyme uptake by acrylic acid-containing microgels indicates that the protein gains one proton as it adsorbs, at a certain solution composition. Our results agree with the experimental finding and suggest that such gain is due to the protonation of the His residue.

The titration curves for the protein amino acids, as well as that of the acid monomers of the gel, are significantly different when adsorbed on the film as compared to the bulk solution. To favor adsorption, the chemical equilibrium of each of these residues is shifted in a non-trivial fashion that depends critically on the particular amino acid. This behavior gives the adsorbed protein flexibility to regulate charge and enhance the electrostatic attractions with the network in a wide range of conditions. Our results show the importance of explicitly accounting for the structure of both network and protein in determining the acid-base equilibrium. Moreover, drawing conclusion from the chemical equilibrium in bulk solution leads to qualitative wrong results as in the nanoconfined adsorbed gel the coupling between the chemical equilibrium and molecular organization leads to emergent behavior.

The charge of the network increases monotonically (but in different measures) with the pH for both pure salt and lysozyme solutions. The thickness of chemically grafted films is a non-monotonic function of the pH. This behavior is the result of the increasing concentration of adsorbed counterions as the network charges, to maintain electroneutrality of the film. The increasing concentration of adsorbed ions has a dual (opposing) effect of screening the intra-network electrostatic repulsions, which disfavors swelling, and at the same time promoting dissociation of the network's acid groups, which favors swelling.

Protein adsorption modifies the swelling transition of the pH-responsive film. The swelling-deswelling behavior observed at intermediate pH for pure salt solutions is more pronounced for lysozyme solutions. The reason is the large volume occupied by adsorbed proteins. As the pH increases, lysozyme reduces its charge, and small Na^+ cations

increasingly replace the protein as the neutralizing species. Thus, the film shrinks with increasing pH in part because the net volume occupied the neutralizing species decreases.

The results presented in this work provide essential molecular information in the design of stimuli-sensitive matrix for chromatography of proteins. For example, the adsorption-release of proteins from adsorbent materials may be reversibly controlled by lowering (or increasing) the salt concentration of the solution, even when the pH is above the protein solution pI. More importantly, our work provides a fundamental understanding of the non-trivial coupling that exists between molecular organization, physical interactions and chemical equilibrium in nanoconfined environments. Further, our work points out to the importance of local environment and specific molecular structure in understanding and predicting chemical reaction equilibrium.

Acknowledgements

This work was supported by a grant from the NSF, CBET-1264696.

References

1. K. Y. Lee and D. J. Mooney, *Chem Rev*, 2001, **101**, 1869-1879.
2. J. D. Ehrick, M. R. Luckett, S. Khatwani, Y. Wei, S. K. Deo, L. G. Bachas and S. Daunert, *Macromol Biosci*, 2009, **9**, 864-868.
3. N. A. Peppas, P. Bures, W. Leobandung and H. Ichikawa, *Eur J Pharm Biopharm*, 2000, **50**, 27-46.
4. P. Gupta, K. Vermani and S. Garg, *Drug Discov Today*, 2002, **7**, 569-579.
5. A. M. Lenhoff, *J Chromatogr A*, 2011, **1218**, 8748-8759.
6. J.-C. Janson, *Protein purification : principles, high resolution methods, and applications*, John Wiley & Sons, Hoboken, N.J., 3rd edn., 2011.
7. X. K. Xu and A. M. Lenhoff, *Journal of Physical Chemistry B*, 2008, **112**, 1028-1040.
8. X. K. Xu and A. M. Lenhoff, *Journal of Chromatography A*, 2009, **1216**, 6177-6195.
9. F. Galisteo and W. Norde, *Colloids and Surfaces B-Biointerfaces*, 1995, **4**, 375-387.
10. B. D. Bowes, H. Koku, K. J. Czymmek and A. M. Lenhoff, *Journal of Chromatography A*, 2009, **1216**, 7774-7784.
11. N. Welsch, A. L. Becker, J. Dzubiella and M. Ballauff, *Soft Matter*, 2012, **8**, 1428-1436.
12. R. A. Latour, *Biointerphases*, 2008, **3**, Fc2-Fc12.
13. L. Zhang and Y. Sun, *Biochemical Engineering Journal*, 2010, **48**, 408-415.
14. F. Carlsson, E. Hyltner, T. Arnebrant, M. Malmsten and P. Linse, *The Journal of Physical Chemistry B*, 2004, **108**, 9871-9881.
15. T. Wei, M. A. Carignano and I. Szleifer, *Langmuir*, 2011, **27**, 12074-12081.
16. T. Wei, M. A. Carignano and I. Szleifer, *J Phys Chem B*, 2012, **116**, 10189-10194.
17. K. Kubiak-Ossowska and P. A. Mulheran, *Langmuir*, 2010, **26**, 7690-7694.
18. K. Kubiak-Ossowska and P. A. Mulheran, *Langmuir*, 2012, **28**, 15577-15585.
19. D. Pellenc, R. A. Bennett, R. J. Green, M. Sperrin and P. A. Mulheran, *Langmuir*, 2008, **24**, 9648-9655.
20. M. C. Vaney, S. Maignan, M. Ries-Kautt and A. Ducruix, *Acta Crystallographica Section D*, 1996, **52**, 505-517.
21. C. Sauter, F. Otalora, J. A. Gavira, O. Vidal, R. Giege and J. M. Garcia-Ruiz, *Acta Crystallogr D Biol Crystallogr*, 2001, **57**, 1119-1126.
22. G. Yu, J. Liu and J. Zhou, *The Journal of Physical Chemistry B*, 2014, **118**, 4451-4460.
23. M. Lund, T. Akesson and B. Jonsson, *Langmuir*, 2005, **21**, 8385-8388.
24. C. H. Evers, T. Andersson, M. Lund and M. Skepo, *Langmuir*, 2012, **28**, 11843-11849.
25. P. M. Biesheuvel, M. van der Veen and W. Norde, *Journal of Physical Chemistry B*, 2005, **109**, 4172-4180.
26. P. M. Biesheuvel and A. Wittemann, *J Phys Chem B*, 2005, **109**, 4209-4214.
27. W. M. de Vos, P. M. Biesheuvel, A. de Keizer, J. M. Kleijn and M. A. C. Stuart, *Langmuir*, 2008, **24**, 6575-6584.

28. W. M. de Vos, F. A. M. Leermakers, A. de Keizer, M. A. C. Stuart and J. M. Kleijn, *Langmuir*, 2010, **26**, 492-259.
29. F. Fang and I. Szleifer, *Proceedings of the National Academy of Sciences of the United States of America*, 2006, **103**, 5769-5774.
30. A. Wittemann and M. Ballauff, *Phys Chem Chem Phys*, 2006, **8**, 5269-5275.
31. G. S. Longo, M. O. d. l. Cruz and I. Szleifer, *Soft Matter*, 2012, **8**, 1344-1354.
32. G. S. Longo, M. Olvera de la Cruz and I. Szleifer, *The Journal of Chemical Physics*, 2014, **141**.
33. I. Szleifer, *Physica A*, 1997, **244**, 370-388.
34. P. Gong, T. Wu, J. Genzer and I. Szleifer, *Macromolecules*, 2007, **40**, 8765-8773.
35. T. McPherson, A. Kidane, I. Szleifer and K. Park, *Langmuir*, 1998, **14**, 176-186.
36. J. Satulovsky, M. A. Carignano and I. Szleifer, *P Natl Acad Sci USA*, 2000, **97**, 9037-9041.
37. C. L. Ren, D. Carvajal, K. R. Shull and I. Szleifer, *Langmuir*, 2009, **25**, 12283-12292.
38. K. H. A. Lau, C. L. Ren, S. H. Park, I. Szleifer and P. B. Messersmith, *Langmuir*, 2012, **28**, 2288-2298.
39. G. S. Longo, M. O. de la Cruz and I. Szleifer, *Langmuir*, 2014, **30**, 15335-15344.
40. A. A. R. Teixeira, M. Lund and F. L. s. B. da Silva, *Journal of Chemical Theory and Computation*, 2010, **6**, 3259-3266.
41. Y. Nozaki and C. Tanford, in *Methods in Enzymology*, ed. C. H. W. Hirs, Academic Press, 1967, vol. Volume 11, pp. 715-734.
42. G. S. Longo, M. O. de la Cruz and I. Szleifer, *Macromolecules*, 2011, **44**, 147-158.
43. P. Gong, J. Genzer and I. Szleifer, *Physical Review Letters*, 2007, **98**.
44. L. R. Wetter and H. F. Deutsch, *Journal of Biological Chemistry*, 1951, **192**, 237-242.

Protein adsorption on pH responsive gels shows emergent behavior due to the coupling between molecular organization, physical interaction and chemcial equilibrium in soft confined materials.